

FIG. 1. Laminar model.

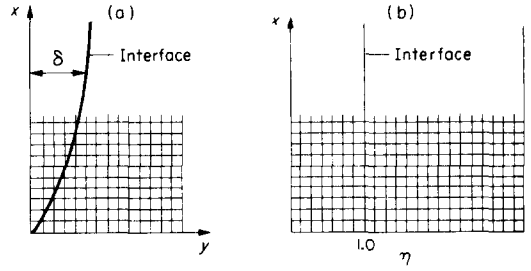


FIG. 2. Grid system.

$$\rho_g C_{p,g} \left[U_g \frac{\partial T_g}{\partial x} + V_g \frac{\partial T_g}{\partial y} \right] = \frac{\partial}{\partial y} \left[K_g \frac{\partial T_g}{\partial y} \right], \quad (3)$$

$$\frac{\partial}{\partial x} (\rho_f U_f) + \frac{\partial}{\partial y} (\rho_f V_f) = 0, \quad (4)$$

$$\rho_f U_f \frac{\partial U_f}{\partial x} + \rho_f V_f \frac{\partial U_f}{\partial y} = g(\rho_\infty - \rho_f) + \frac{\partial}{\partial y} \left[\mu_f \frac{\partial U_f}{\partial y} \right], \quad (5)$$

$$\rho_f C_{p,f} \left[U_f \frac{\partial T_f}{\partial x} + V_f \frac{\partial T_f}{\partial y} \right] = \frac{\partial}{\partial y} \left[K_f \frac{\partial T_f}{\partial y} \right]. \quad (6)$$

Interface conditions

$$U_g = U_f \quad \text{at} \quad y = \delta, \quad (7)$$

$$\mu_g \frac{\partial U_g}{\partial y} = \mu_f \frac{\partial U_f}{\partial y} \quad \text{at} \quad y = \delta, \quad (8)$$

$$T_g = T_f = T_{sat} \quad \text{at} \quad y = \delta, \quad (9)$$

$$\rho_g \left[V_g - U_g \frac{d\delta}{dx} \right] = \rho_f \left[V_f - U_f \frac{d\delta}{dx} \right] \quad \text{at} \quad y = \delta, \quad (10)$$

$$\begin{aligned} & -K_g \frac{\partial T_g}{\partial y} + \epsilon_w \sigma (T_w^4 - T_{sat}^4) \\ & = -K_f \frac{\partial T_f}{\partial y} - \rho_g \left(V_g - U_g \frac{d\delta}{dx} \right) h_{fg} \quad \text{at} \quad y = \delta. \end{aligned} \quad (11)$$

Boundary conditions

$$\left. \begin{aligned} U_g &= 0 \quad \text{at} \quad y = 0, \\ V_g &= 0 \quad \text{at} \quad y = 0, \end{aligned} \right\} \quad (12)$$

$$T_g = T_w \quad \text{at} \quad y = 0, \quad (13)$$

$$U_f \rightarrow 0 \quad \text{as} \quad y \rightarrow \infty, \quad (14)$$

$$T_f \rightarrow T_\infty \quad \text{as} \quad y \rightarrow \infty. \quad (15)$$

We have assumed that the liquid surface acts like a blackbody and that the vapour layer does not participate in radiative transfer. Although fluids like water vapour are strong absorbers in the infrared, the thickness of the vapour layer is usually small and hence the attenuation of radiation from the surface is very small.

NUMERICAL METHOD

The governing equations are parabolic in the x -direction and hence a marching technique would have been the most efficient method to solve the equations. An attempt by Sabhapathy [4] to solve these equations by the marching technique was unsuccessful on account of numerical instabilities. We have solved the finite-difference form of the above equations by the false-transient method.* This approach gives a better physical insight into the nature of the interaction between the two phases.

The presence of a curved liquid-vapour interface suggests the modification of x - y coordinate system to one in which the interface is a part of the grid system. This can be achieved if we use $\eta = y/\delta$ (where δ is the thickness of the vapour layer) as a cross-stream coordinate then $\eta = 1$ always corresponds to the liquid-vapour interface (see Fig. 2). The basic conservation equations are transformed from the x - y to the x - η system and are given below. The unsteady terms have been introduced in momentum, energy and interface energy balance equations to facilitate the use of the false-transient method.

Conservation equations (x - η system)

$$\frac{\partial}{\partial x} (\rho_g U_g) - \frac{\partial}{\partial \eta} (\rho_g U_g) \frac{\eta}{\delta} \frac{d\delta}{dx} + \frac{1}{\delta} \frac{\partial}{\partial \eta} (\rho_g V_g) = 0, \quad (16)$$

$$\begin{aligned} & \rho_g \left[\frac{\partial U_g}{\partial t} + U_g \frac{\partial U_g}{\partial x} - U_g \frac{\partial U_g}{\partial \eta} \frac{\eta}{\delta} \frac{d\delta}{dx} + \frac{V_g}{\delta} \frac{\partial U_g}{\partial \eta} \right] \\ & = g(\rho_\infty - \rho_g) + \frac{1}{\delta} \frac{\partial}{\partial \eta} \left(\frac{\mu_g}{\delta} \frac{\partial U_g}{\partial \eta} \right), \end{aligned} \quad (17)$$

$$\begin{aligned} & \rho_g C_{p,g} \left[\frac{\partial T_g}{\partial t} + U_g \frac{\partial T_g}{\partial x} - U_g \frac{\partial T_g}{\partial \eta} \frac{\eta}{\delta} \frac{d\delta}{dx} + \frac{V_g}{\delta} \frac{\partial T_g}{\partial \eta} \right] \\ & = \frac{1}{\delta} \frac{\partial}{\partial \eta} \left(\frac{K_g}{\delta} \frac{\partial T_g}{\partial \eta} \right), \end{aligned} \quad (18)$$

$$\frac{\partial}{\partial x} (\rho_f U_f) - \frac{\partial}{\partial \eta} (\rho_f U_f) \frac{\eta}{\delta} \frac{d\delta}{dx} + \frac{1}{\delta} \frac{\partial}{\partial \eta} (\rho_f V_f) = 0, \quad (19)$$

* By 'false-transient method' we mean that transient terms are introduced only in some equations and hence the new equations do not represent the true unsteady conservation equations.

$$\rho_f \left[\frac{\partial U_f}{\partial t} + U_f \frac{\partial U_f}{\partial x} - U_f \frac{\partial U_f}{\partial \eta} \frac{\eta}{\delta} \frac{d\delta}{dx} + \frac{V_f}{\delta} \frac{\partial U_f}{\partial \eta} \right] = g(\rho_\infty - \rho_f) + \frac{1}{\delta} \frac{\partial}{\partial \eta} \left(\mu_f \frac{\partial U_g}{\partial \eta} \right), \quad (20)$$

$$\rho_f C_{p,f} \left[\frac{\partial T_f}{\partial t} + U_f \frac{\partial T_f}{\partial x} - U_f \frac{\partial T_f}{\partial \eta} \frac{\eta}{\delta} \frac{d\delta}{dx} + \frac{V_f}{\delta} \frac{\partial T_f}{\partial \eta} \right] = \frac{1}{\delta} \frac{\partial}{\partial \eta} \left(K_f \frac{\partial T_f}{\partial \eta} \right). \quad (21)$$

Interface conditions

$$U_g = U_f \quad \text{at} \quad \eta = 1, \quad (22)$$

$$\mu_g \frac{\partial U_g}{\partial \eta} = \mu_f \frac{\partial U_f}{\partial \eta} \quad \text{at} \quad \eta = 1, \quad (23)$$

$$T_g = T_f = T_{\text{sat}} \quad \text{at} \quad \eta = 1, \quad (24)$$

$$\rho_g \left(V_g - U_g \frac{d\delta}{dx} \right) = \rho_f \left[V_f - U_f \frac{d\delta}{dx} \right] \quad \text{at} \quad \eta = 1, \quad (25)$$

$$- \frac{K_g}{\delta} \left(\frac{\partial T_g}{\partial \eta} \right) + \varepsilon_w \sigma (T_w^4 - T_{\text{sat}}^4) = - \frac{K_f}{\delta} \frac{\partial T_f}{\partial \eta} - \rho_g \left(V_g - U_g \frac{d\delta}{dx} + \frac{d\delta}{dt} \right) h_{fg} \quad \text{at} \quad \eta = 1. \quad (26)$$

Boundary conditions

$$U_g = 0 \quad \text{at} \quad \eta = 0, \quad (27)$$

$$T_g = T_w \quad \text{at} \quad \eta = 0, \quad (28)$$

$$U_f \rightarrow 0 \quad \text{as} \quad \eta \rightarrow \infty, \quad (29)$$

$$T_f \rightarrow T_\infty \quad \text{as} \quad \eta \rightarrow \infty. \quad (30)$$

FINITE-DIFFERENCE PROCEDURE

The central-difference scheme is used for all space derivatives except the convection terms in momentum and energy equations. For the latter the upwind-difference scheme is used. For time derivatives the explicit scheme is used. There are six variables (U_g , V_g , U_f , V_f , T_g , and T_f) in the vapour and liquid regions and three interface parameters (U_f , V_f , and δ) which need to be determined at each new time level. The sequence of advancement from the old time level to the new time level is as follows:

(1) The velocity of the vapour/liquid in the x -direction (U_g/U_f) is evaluated from the finite-difference form of the vapour/liquid momentum equation [equation (17)/(20)].

(2) The velocity of the vapour/liquid in the y -direction (V_g/V_f) is evaluated from the finite-difference form of the vapour/liquid mass conservation equation [equation (16)/(19)].

(3) The temperature of the vapour/liquid is evaluated from the finite-difference form of vapour/liquid energy equation [equation (18)/(21)].

(4) The thickness of the vapour layer was evaluated from the finite-difference form of the interface energy balance [equation (26)].

(5) The velocity of the liquid or vapour at the interface in the x -direction was evaluated from the finite-difference form of the interface shear stress balance [equation (23)].

(6) The velocity of the liquid at the interface in the y -direction was evaluated from the finite-difference form of the interface mass balance [equation (25)].

The number of grid points in the x - and η -direction were K and M , respectively. The choice of M depends upon the thickness of the liquid boundary layer. We found that a choice of $M = 40$ was adequate on the basis of the analytical work of Frederking and Hopfenfeld [5]. The number of grid points within the vapour region was chosen to be 10. The number of grid points needed in the x -direction depends upon the grid size and also how far from the leading edge numerical results are required. We chose the grid size in the x -direction to be 1 mm and the number of grid points to be 15.

This meant that results were obtained only up to 1.5 cm from the leading edge. It is not useful to go beyond this height because the flow generally becomes turbulent. Although 1.5 cm may be seen to be an unrealistically small height the results obtained here can be compared with experimental data on film boiling from wires. If the wire diameter is greater than 10 mm curvature effects can be neglected.

With 15 grid points in the x -direction and 40 in the η -direction we have a total of 600 grid points. It is not necessary to iterate the equations at all the 600 grid points simultaneously. We can exploit the fact that the equations are parabolic in the x -direction by first iterating the variables at grid points close to the leading edge to steady state and then using these values for iteration of variables at grid points away from the leading edge. Hence the variables at 40 grid points at the first x location ($I = 1$) were iterated till steady state was reached. The variables at the next x location ($I = 2$) were iterated next using the steady-state values at $I = 1$. The above method ensures a faster convergence than would be achieved by iterating the variables at all grid points simultaneously.

The finite-difference equations converge rapidly to the steady-state value if a judicious choice of initial profile of velocity and temperature are made. The initial velocity of the vapour in the x -direction and the vapour layer thickness was chosen to be that given by Bromley [1]. The initial velocity profile had a zero interfacial velocity. This was preferred to the profile with zero interfacial stress because in the latter case there is no sure way of ensuring that momentum is transferred to the liquid layer as the equations are iterated (for details see Rao [7]).

The initial temperature profile in the vapour region was chosen to be linear. The initial velocity in the x -direction and the initial temperature in the liquid

were chosen to have parabolic profiles. The velocity in the y -direction in the vapour and liquid were derived from the continuity equations.

The most commonly used criterion for ascertaining when an iteration can be terminated is the relative error criterion. The relative criterion can be stated as

$$\max_{ij} \left| \frac{W_{ij}^{n+1} - W_{ij}^n}{W_{ij}^n} \right| \leq \varepsilon; \quad W_{ij}^n \neq 0.$$

Here W_{ij} is any variable like velocity or temperature at the grid point i, j , at time n . This criterion is not suitable for the present problem for the following reason. The explicit false-transient method used here restricts the time step to very small values to avoid numerical instability. For such small time steps there is very little change in variable from one time step to the next and hence the above criterion can be satisfied easily well before actual steady state is reached.

A better method is to compare the transient terms introduced in the conservation equations with other terms in those equations. When the transient term is less than 1% of the most significant term in the equation then one can assume that steady state has been reached. It is important to compare the transient term with the most significant term in the equation because the other terms in the equation may be insignificant under certain conditions. The new criterion can be stated as

$$\max_{ij} \left| \frac{W_{ij}^{n+1} - W_{ij}^n}{\Delta t} \right| < \frac{\text{Most significant term}}{100}.$$

As already mentioned, the explicit false-transient method used here restricts the time step to very small values, on account of numerical instability. The time step that can be chosen without encountering

instability can be determined by trial and error. Typically the time step had to be kept below $20 \mu\text{s}$ to ensure freedom from numerical instabilities. This limitation on the time step is imposed by conditions in the vapour region. This can be conjectured by applying the criterion for stability in a single phase flow to the vapour region [6]. With a time step of $20 \mu\text{s}$, the finite-difference equations required around 20 000 iterations to reach the steady state. Such a large number of iterations are required because the liquid, which has a large inertia, responds very slowly. The convergence in the liquid region can be accelerated by the use of the technique of over-relaxation. The over-relaxation technique can be stated as

$$U_{ij}^{n+1} = U_{ij}^n + \phi \Delta t \quad [\text{contribution due to convection, diffusion and buoyancy terms}],$$

where U is the x -direction velocity or temperature in the liquid region and ϕ is the relaxation parameter. When ϕ values were chosen in the range 100–400 (depending upon the degree of superheating and subcooling) it was found that the finite-difference equations converged to the steady state in about 2000 iterations. The technique of over-relaxation can be thought of as an artificial reduction of the inertia of the liquid. Such an artificial reduction is possible in the false-transient method because we are interested only in the steady-state solution. With a total of 600 grid points the present numerical scheme took 4 min of CPU time for saturated film boiling and about 8 min for subcooled film boiling. Of the total time taken around 3 min were consumed in the calculation of physical properties as a function of temperature.

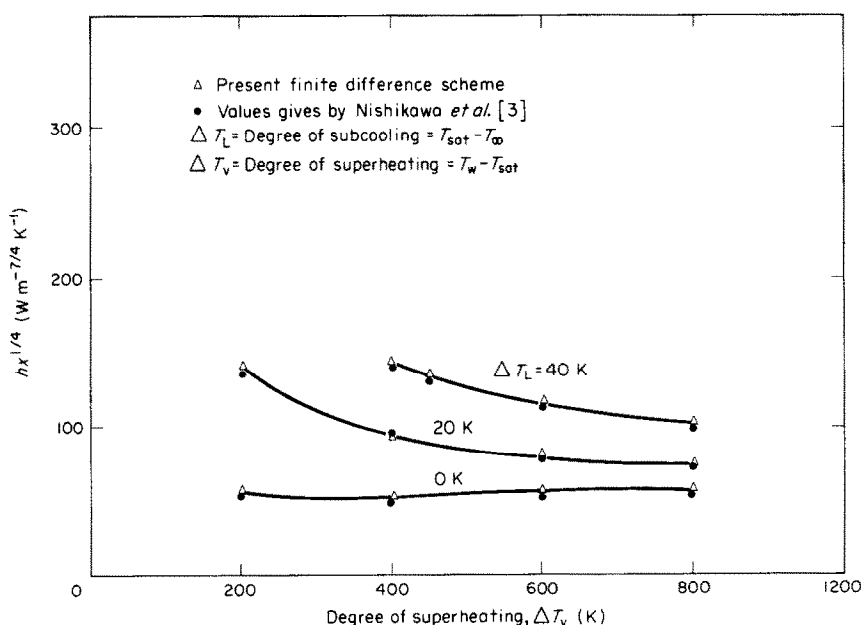


FIG. 3. Comparison of heat transfer coefficient with the values given by Nishikawa *et al.* [3].

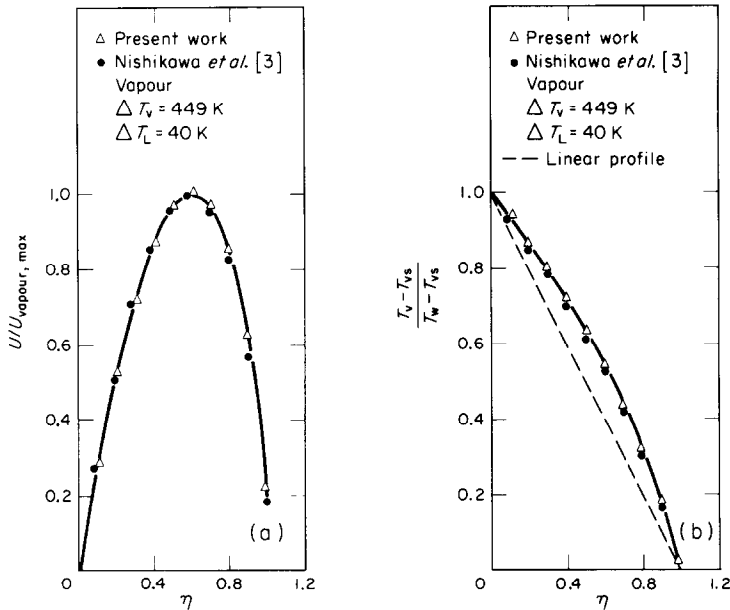


FIG. 4. Comparison of velocity and temperature profile in vapour region.

RESULTS

The numerical method developed in this paper was used to study laminar film boiling from a vertical plate for water at atmospheric pressure and with various degrees of superheating and subcooling. We will first compare our results with those obtained by Nishikawa *et al.* [3]. To do so, we must first ignore the role of radiation. With the emissivity of the plate assumed to be

zero, the results obtained with the present numerical scheme should agree with those of Nishikawa *et al.* [3], who used the Runge–Kutta method. Figure 3 shows the variation of $hx^{1/4}$ (which is constant in this case) as a function of the degree of superheating and subcooling. We find that the results obtained by the present numerical scheme agree very well with those obtained by Nishikawa *et al.* [3]. Figures 4(a) and (b) compare the velocity in the x-direction and temperature in the

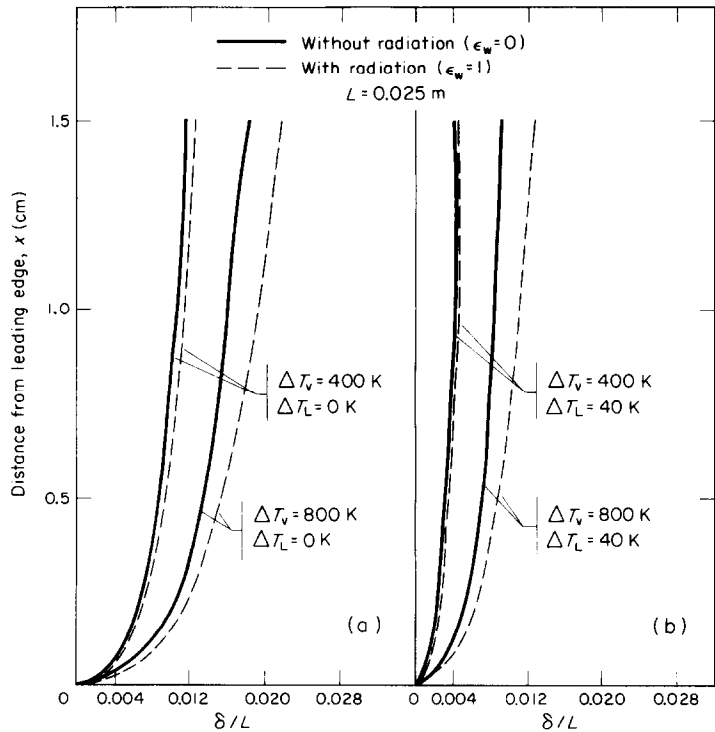


FIG. 5. Variation of vapour layer thickness with x.

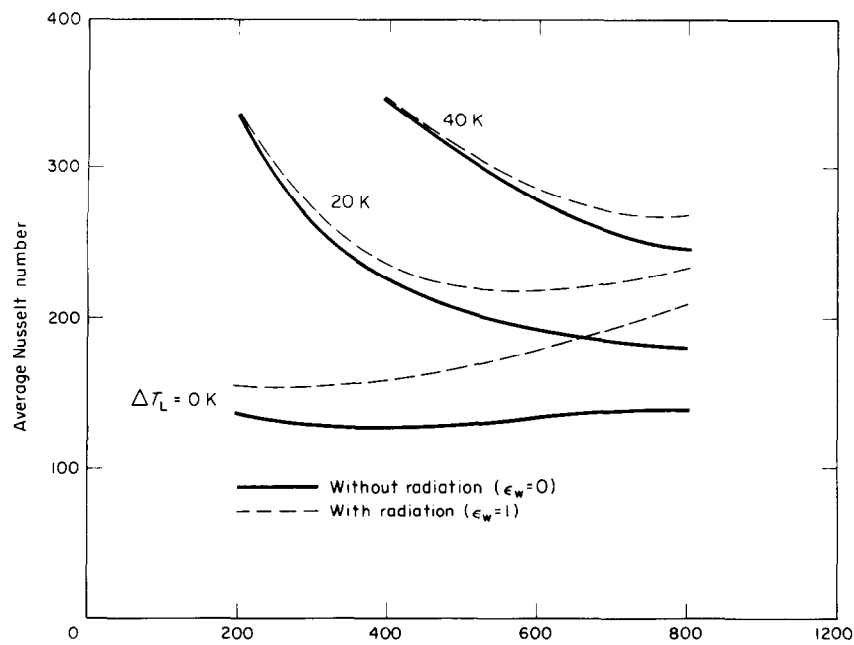


FIG. 6. Effect of radiation on average Nusselt number.

vapour region as obtained by the two methods. Once again the agreement is very good. We can now say that the choice of grid and the number of grid points in the present numerical scheme were adequate to give accurate results.

The presence of surface radiation influences the heat

transfer in laminar film boiling in two different ways : (1) it provides an alternative path for heat transfer from the surface to the interface ; (2) it reduces the convective heat transfer by increasing the thickness of the vapour layer. Figures 5(a) and (b) show the effect of radiation on the thickness of the vapour layer. The effect of radiation

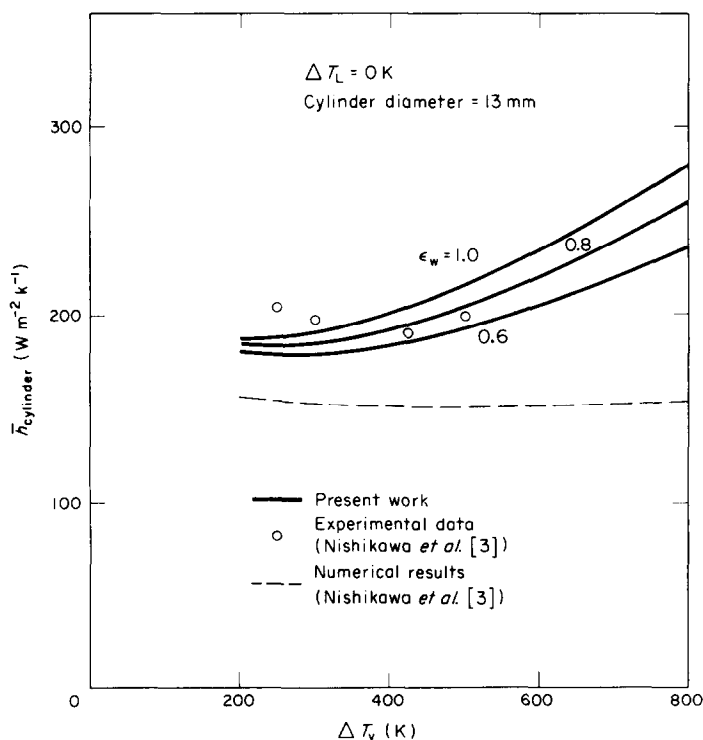


FIG. 7. Comparison of present results with experimental data.

on vapour layer thickness is more in saturated film boiling than in subcooled film boiling because, in the latter, most of the energy is used to heat up the subcooled liquid. The effect of radiation on the mean Nusselt number is shown in Fig. 6. We see that radiation plays an important role when the degree of superheating of the surface is high and the degree of subcooling of the ambient liquid is low.

Finally we compare results of the present numerical computations with experimental data. Experimental data on laminar film boiling is available for thin wires in water. We can apply the results obtained here (for a semi-infinite plate) to a cylindrical geometry provided the vapour layer thickness is small compared to the radius of the cylinder. Hence we can use the results obtained for a semi-infinite plate (after accounting for variation in the acceleration due to gravity, in the cylindrical geometry) if the cylinder diameter is greater than 10 mm. In Fig. 7, the results of the present computations and those of Nishikawa *et al.* [3] are compared with experimental data of Nishikawa *et al.* [3]. Since the emissivity of the wire used in the experiment was not known results are shown for a range of emissivities between 0.6 and 1. We see that the inclusion of radiation in the present computations has resulted in a better agreement with experimental data. The experimental data show an increase in heat transfer coefficient when the cylinder temperature is less than 300 K above the saturation temperature. This may be on account of unstable film boiling which can occur when the cylinder temperature is not very high.

CONCLUSION

The basic conservation equations in laminar film boiling can be solved numerically by the false-transient method. The convergence of the finite-difference equations on the liquid side can be accelerated by the use of the technique of over-relaxation. The effect of radiation cannot be neglected in the evaluation of heat transfer from the plate. The criterion for determining whether steady state has been reached must be chosen carefully. It should be based on the contribution of unsteady terms in the basic conservation equations.

REFERENCES

1. L. Bromley, Heat transfer in stable film boiling, *Chem. Engng Prog.* **46**(5), 221-227 (1950).
2. E. K. Kalinin, I. I. Berlin and V. V. Kostuk, Film-boiling heat transfer, *Adv. Heat Transfer* **11**, 51-197 (1975).
3. K. Nishikawa, T. Ito and K. Matsumoto, Investigation of variable thermophysical problem concerning pool film boiling from vertical plate with prescribed uniform temperature, *Int. J. Heat Mass Transfer* **19**, 1175-1181 (1976).
4. P. Sabhapathy, Numerical study of radiative effects in film boiling from a vertical plate, M.Tech. thesis, Department of Mechanical Engineering, Indian Institute of Technology, Kanpur (1980).
5. T. N. K. Frederking and J. Hopenfeld, Laminar two-phase boundary layers in natural convection film boiling of a subcooled liquid, *Z. Angew Math. Phys.* **15**, 388-399 (1964).
6. P. J. Roache, *Computational Fluid Dynamics* (revised edn.). Hermosa, Albuquerque, U.S.A. (1976).
7. N. S. Rao, Numerical study of laminar film boiling by finite difference method, M.Tech. thesis, Department of Mechanical Engineering, Indian Institute of Technology, Kanpur (1981).

ETUDE NUMERIQUE PAR LA METHODE AUX DIFFERENCES FINIES DU TRANSFERT THERMIQUE DANS L'EBULLITION EN FILM LAMINAIRE

Résumé— La forme aux différences finies des équations fondamentales de conservation pour l'ébullition en film laminaire a été traitée par la méthode de fausse transition. Par un choix judicieux du système de coordonnées, l'interface vapeur-liquide se prête au système de grille. Une différenciation centrée est utilisée pour les termes de diffusion, une différenciation courante pour les termes de convection, et une différenciation explicite pour les termes transitoires. Puisque une méthode explicite est utilisée, le pas de temps dans la méthode de fausse transition est limité par l'instabilité numérique. Dans le problème étudié, les limites du pas de temps sont imposées par des conditions dans la région de vapeur. D'autre part la vitesse de convergence dépend des conditions dans la région liquide. La vitesse de convergence est accélérée par l'utilisation de la technique de sur-relaxation dans la région liquide. Les résultats obtenus se comparent bien avec un travail antérieur et des données expérimentales disponibles dans des publications.

NUMERISCHE UNTERSUCHUNG DER WÄRMEÜBERTRAGUNG BEIM LAMINAREN FILMSIEDEN MIT DER FINITEN-DIFFERENZEN-METHODE

Zusammenfassung—Die Erhaltungsgleichungen beim laminaren Filmsieden wurden in finiter Differenzenform quasistationär gelöst. Durch eine geeignete Wahl des Koordinatensystems wurde die Dampf/Flüssigkeitsgrenzfläche in das Gitternetz eingepaßt. Für die Diffusionsglieder wurden zentrale Differenzen, für die Konvektionsglieder Vorwärtsdifferenzen und für die instationären Glieder explizite Differenzen verwendet. Da eine explizite Methode verwendet wird, wird die Größe des Zeitschritts in dem quasistationären Verfahren durch numerische Instabilität begrenzt. In dem hier vorliegenden Problem sind die Grenzen des Zeitschritts durch Bedingungen im Dampfgebiet gegeben. Andererseits ist die Konvergenzgeschwindigkeit der finiten Differenzengleichungen von den Bedingungen im Flüssigkeitsgebiet abhängig. Die Konvergenzgeschwindigkeit wurde durch die Anwendung der Überrelaxationsmethode im Flüssigkeitsgebiet beschleunigt. Die erhaltenen Ergebnisse stimmen gut mit vorherigen Arbeiten und experimentellen Daten aus der Literatur überein.

**ЧИСЛЕННОЕ ИССЛЕДОВАНИЕ ТЕПЛОПЕРЕНОСА ПРИ
ЛАМИНАРНОМ ПЛЕНОЧНОМ КИПЕНИИ МЕТОДОМ КОНЕЧНЫХ РАЗНОСТЕЙ**

Аннотация—С помощью метода установления получено решение основных уравнений сохранения в конечно-разностном виде, описывающих ламинарное пленочное течение. Соответствующим выбором системы координат граница раздела пар-жидкость фиксировалась на расчетной сетке. Для диффузионных членов использовались центральные разностные производные, для конвективных – правые разностные производные, а дифференцированием в явном виде определялись члены, учитывающие нестационарность процесса. В связи с использованием явного метода временной шаг метода установления ограничен численной неустойчивостью. В рассматриваемой задаче ограничения на временной шаг налагаются условиями в области пара. С другой стороны, скорость сходимости конечно-разностных уравнений зависит от условий в области жидкости. Сходимость ускоряется за счет использования метода верхней релаксации в жидкой фазе. Полученные результаты хорошо согласуются с результатами предыдущей работы и с имеющимися в литературе экспериментальными данными.